

## SOURCE-DEPENDENT PROBABILITY DENSITIES EXPLAINING FREQUENCY DISTRIBUTIONS OF AMBIENT DOSE RATE IN THE NETHERLANDS

R. C. G. M. Smetsers and R. O. Blaauboer  
National Institute of Public Health and the Environment (RIVM)  
Laboratory of Radiation Research  
PO Box 1, 3720 BA Bilthoven, The Netherlands

*Received April 23 1996, Accepted May 29 1996*

**Abstract** — Several sources and processes contribute to the natural radiation background level, causing significant fluctuations in time. Quantified knowledge on the probability of these variations is desirable for many reasons, e.g. to discriminate between natural and human-induced factors or to support the management of nuclear emergency networks. Frequency distributions of ambient dose rate, as observed by the Dutch National Radioactivity Monitoring Network over the period 1990–1994, have been explained through the joint contribution of five time-varying sources, including counting statistics. Normalised probability density functions (with a normal shape for noise, terrestrial and cosmogenic radiation, and an exponential shape for airborne and deposited radioactivity from radon progeny) add up to one joint probability density function, which agrees with long-term data distributions over four orders of magnitude. This comparison yields parameter values describing the probable impact of rainout and washout of radon progeny and the typical fluctuation band of terrestrial radiation as observed in the Netherlands.

### INTRODUCTION

A research programme aimed at obtaining quantified descriptions of the processes responsible for variations in natural radioactivity and radiation levels in the Netherlands is currently in operation at the RIVM<sup>(1)</sup>. The experimental data necessary for this study — which are supposed to have adequate resolution in space and time — are obtained from the Dutch National Radioactivity Monitoring network (NRM)<sup>(2)</sup>. A major part of this programme involves the assessment of ambient dose rates. In a recent paper, an analysis on time-series yielded quantified information on the various processes and sources contributing to the natural background in the Dutch outdoor environment<sup>(3)</sup>. It was shown that most of the observed temporal variations could be explained by variations in airborne concentrations of <sup>222</sup>Rn progeny, precipitation and air pressure, and simplified expressions were presented to estimate the natural background within a small uncertainty range. Other parameters, such as the radon soil profile and the cosmogenic source strength, were found to be less influential. These findings were adequate to provide a dynamic compensation method for natural background radiation; however, they do not provide all the information needed to estimate the range and distribution of ambient dose rate data likely to be observed over a long period of time. Knowledge of this kind not only classifies the impact of various sources and processes on variations in outdoor radiation levels, but is also desired, for instance, to establish sensitive warning levels in automated emergency networks<sup>(1,2)</sup>.

To compensate for this lack of information, the element of probability is taken into account. This paper

will propose simple probability density functions for the various sources contributing to the ambient dose rate in the Netherlands so as to predict the likelihood of dose rate contributions over a long period of time, e.g. one year. These source-specific probability densities are merged into one joint probability density function, which is compared to annual frequency distributions of dose rate, as recorded by the NRM (see Figure 1). This approach is believed to make sense; firstly, because location dependent annual average values of ambient dose rate remain very stable over the years<sup>(1,4)</sup>, and secondly, because frequency distributions obtained from various locations and years (see Figure 2) show a remarkable similarity in shape. More than 20 annual data histograms were analysed, yielding distribution functions and parameter values and describing the influence of each relevant natural source on the range of ambient dose rate data in the Netherlands.

### INSTRUMENTATION

Radiological data are obtained from the NRM. Measurements of external irradiation levels (at 58 locations) and airborne radioactivity (at 14 locations) are recorded every 10 min and stored in a relational database. NRM locations are identified by their names, followed by three digits in brackets, like 'Wijnandsrade (133)'. Technical specifications of the network, including location numbers and positions, and the performance it shows as an emergency network, are found elsewhere<sup>(2)</sup>. NRM recordings were shown to meet the requirements of examining small variations in natural background radiation levels as they occur in the

Netherlands<sup>(1,4,5)</sup>; technical information presented here is therefore restricted to the essentials.

For the monitoring of external irradiation levels the NRM is equipped with proportional counters (Bitt Technology Inc.), RS02 tube with an accessory RM10E readout unit<sup>(6)</sup>. Recordings are converted to the dosimetric quantity ambient dose-equivalent rate at 10 mm depth,  $\dot{H}^*(10)$ <sup>(7)</sup> which is further abbreviated to (ambient) dose rate. The NRM dose rate meters hold some systematic errors (for instance, they overestimate the cosmogenic dose rate), but these errors are correctable and do not affect the dynamic response of the equipment<sup>(4)</sup>. The reproducibility and mutual interchangeability of the applied radiation counters were shown to be very satisfactory; the accuracy of the data is, apart from counting statistics, estimated at 1% ( $1\sigma_{rel}$ ) for typical background levels<sup>(1,4)</sup>. The counter tubes are mounted 1 m above the rooftop of the NRM measuring cabins, about 3.5 m above ground level. Although most NRM locations are found in rural areas, recordings of ambient dose rate are influenced by the presence of pavements or small structures in the vicinity of the measuring sites<sup>(4,8)</sup>.

Recordings of airborne radioactivity are conducted using a moving-tape air sampler (FAG Kugelfischer Georg Schäfer KGaA FRG, type: FHT 59S<sup>(9)</sup>). It was shown<sup>(5)</sup> that recordings of natural gross  $\alpha$  activity concentrations in air can be converted to the actual equilibrium-equivalent decay product concentration of  $^{222}\text{Rn}$ , EEDC<sup>(10)</sup>. The total uncertainty ( $1\sigma_{rel}$ ) in the determination of the EEDC is estimated at 12%. Any contribution of  $^{220}\text{Rn}$  progeny to the initial recordings

can be neglected for various reasons, one of them being the air sampling height of almost 5 m<sup>(5)</sup>.

Meteorological data are supplied by the Royal Netherlands Meteorological Institute (KNMI).

## METHOD

Consider an arbitrary normalised probability density function,  $U(\gamma)$ , expressing the probability that a certain source or process yields a contribution to the ambient dose rate,  $\gamma$ , between  $\gamma$  and  $\gamma + d\gamma$ . Next, consider two such probability density functions,  $U(\gamma)$  and  $V(\gamma)$ , describing the probable contributions of two (uncorrelated) sources. The function  $W(\gamma)$ , representing the 'probable sum' of these independent sources, is calculated as follows:

$$W(\gamma) = \int_{-\infty}^{\infty} U(\xi) V(\gamma - \xi) d\xi \quad (1)$$

If  $U(\gamma)$  and  $V(\gamma)$  are both normal distributions,  $W(\gamma)$  is also normally shaped, having a mean value  $\mu \equiv \gamma_w = \gamma_U + \gamma_V$  and a standard deviation  $\sigma \equiv \sigma_w = (\sigma_U^2 + \sigma_V^2)^{1/2}$ . We will apply this result to the dose rate contributions from cosmogenic and terrestrial radiation, which we assume to be normally distributed. The influence of counting statistics on recorded data can also be described by a normal distribution; in this approach, we treat 'counting statistics' as the third 'normally distributed (virtual) radiation source'. The contributions from these three 'sources' are thus easily combined. However, dose rates due to airborne and deposited  $\gamma$ -emitters

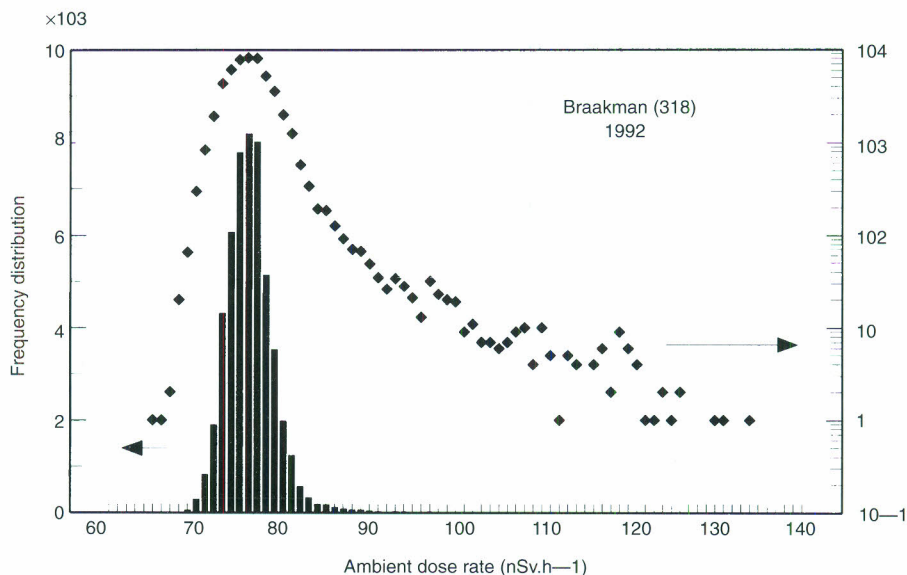


Figure 1. Frequency distribution of over 50,000 pieces of ambient dose rate data (10 min sampling period) recorded at Braakman (318) in 1992. The histogram (1 nSv.h<sup>-1</sup> intervals) looks normal on a linear scale (bars) but presentation on a logarithmic scale (symbols) shows a tail of elevated data due to the washout of  $^{222}\text{Rn}$  progeny.

from the  $^{222}\text{Rn}$  decay series are far from normally distributed. Their probability densities will therefore be approximated by differently shaped functions and Equation 1 will have to be used again to incorporate the influence of these sources to the joint probability density function.

### Cosmogenic radiation

Approximately half of the ambient dose rate present in the Netherlands originates from secondary cosmic radiation. Temporal variations in this contribution are primarily explained by variations in air pressure. Variations in the cosmogenic source strength are believed to be low at sea level<sup>(11)</sup>. This assumption is confirmed by six years of NRM observations, with one exception, i.e. in summer 1991, when a significant signal drop was observed at all NRM locations<sup>(3,4)</sup>. For the Netherlands, any dependence on altitude and geographic latitude is not of importance for this work.

The relationship between air pressure and ambient dose rate was shown to be linear in the typical air pressure range observed at sea level. The corresponding coefficient of proportionality,  $C_p$ , was found to be  $-0.120 \pm 0.003$  ( $1\sigma$ )  $\text{nSv}\cdot\text{h}^{-1}\cdot\text{hPa}^{-1}$ <sup>(3,4)</sup>. Hence, the probability density function of the cosmic ray contribution conforms to the air pressure distribution. Long-range air pressure data are available, showing fairly normal shaped distributions. The long-term average value for the Netherlands is 1015 hPa but annual average values vary between 1012 and 1018 hPa<sup>(12)</sup>. The stan-

dard deviation of an annual distribution,  $\sigma_p$ , is typically 10 hPa. The cosmogenic probability density function,  $C(\gamma)$ , can thus be approximated by a normal distribution with shape parameters  $\mu \equiv \gamma_C$  and  $\sigma \equiv \sigma_C$ . At standard air pressure (1013 hPa), the average cosmogenic contribution to the ambient dose rate is estimated at  $40 \text{ nSv}\cdot\text{h}^{-1}$ <sup>(4,11)</sup>. The standard deviation is calculated as the product of  $C_p$  and  $\sigma_p$ , yielding  $\sigma_C = 1.20 \text{ nSv}\cdot\text{h}^{-1}$ , with an estimated uncertainty of  $0.10 \text{ nSv}\cdot\text{h}^{-1}$ .

### Terrestrial radiation

Gamma radiation from primordial radionuclides in soil (and building materials) forms the second most significant contribution to the ambient dose rate. This contribution is strongly location-dependent due to different soil types. Some of the most important radionuclides in this context are short-lived decay products of a radon isotope (e.g.  $^{214}\text{Bi}$ ,  $^{214}\text{Pb}$  and  $^{208}\text{Tl}$ ). One may therefore expect the terrestrial component to show fluctuations in time as a result of temporal variations in the radon soil profile<sup>(4,8,13,14)</sup>. However, from the analysis of time-series these variations seem fairly low in the Netherlands<sup>(3,4)</sup>. In this approach, the terrestrial probability density function (including possible effects of the built-up environment) is represented by a normal distribution, with a location-dependent mean value,  $\gamma_T$ , in the range of  $15\text{--}75 \text{ nSv}\cdot\text{h}^{-1}$  and a presumably small standard deviation,  $\sigma_T$ , yet to be determined.

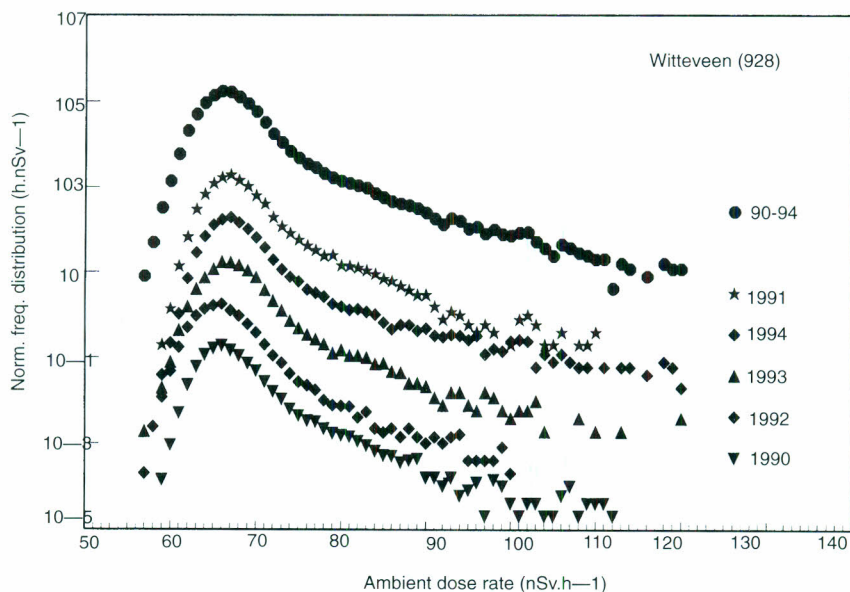


Figure 2. Normalised annual frequency distributions of ambient dose rate (10 min sampling time) observed at Witteveen (928) over the period 1990–1994. The distributions for 199x ( $x = 0\text{--}4$ ) are multiplied by a factor of  $10^x$ , leaving the 1990 distribution on a proper scale. The top distribution multiplied by  $10^6$  is obtained from the complete data set.

### Counting statistics

Radiation data are generally affected by counting statistics. Nuclear decay obeys Poisson statistics and the associated short-term temporal variations in radiation data are, in general, normally distributed around the average value, with a relative standard deviation equal to  $n^{-1/2}$ ,  $n$  being the (average) number of counts received in one sampling period. For this to be true demands the registration of photon counts to be uncorrelated. In our case, this assumption seems valid due to the very small geometric detection efficiency of the counter tube and the applied sampling time of 10 min, which is short when compared to the half-lives of the short-lived  $\gamma$ -emitting radionuclides of the  $^{220}\text{Rn}$  and  $^{222}\text{Rn}$  decay chains. Counting statistics can thus be regarded as a 'virtual' radiation source with a normal probability density function,  $N(\gamma)$ , with shaping parameters  $\mu \equiv \gamma_N = 0$  and  $\sigma \equiv \sigma_N = \gamma_{\text{avg}} n^{-1/2} = \gamma_{\text{avg}}^{1/2} N_0^{-1/2}$ . The parameter  $N_0$  stands for the average number of counts registered per unit dose rate per sampling period. For the equipment used,  $N_0$  was found to be 29 counts per  $\text{nSv}\cdot\text{h}^{-1}$  per 10 min<sup>(4)</sup>.

Based on the above, the probability density function  $S(\gamma)$  describing the joint contribution from counting statistics, cosmogenic and terrestrial radiation to the ambient dose rate is thus represented by a normal distribution, where the mean  $\gamma_S = \gamma_C + \gamma_T$  and the standard deviation  $\sigma_S = (\sigma_C^2 + \sigma_T^2 + \sigma_N^2)^{1/2}$ . Two of the five parameters, i.e.  $\gamma_T$  and  $\sigma_T$ , are free and yet have to be determined from measured frequency distributions.

### Airborne radioactivity

The contribution of airborne radioactivity to the ambient dose rate is dominated by  $\gamma$  radiation from two short-lived  $^{222}\text{Rn}$  decay products,  $^{214}\text{Bi}$  and  $^{214}\text{Pb}$ ; it is assumed to be linearly proportional to the concentration of the equilibrium equivalent decay product concentration of  $^{222}\text{Rn}$  in air, EEDC. The EEDC values are independently measured from the ambient dose rate by the FAG FHT59S monitors of the NRM<sup>(2,5)</sup>, and the probability function of this source can thus be deduced from the measured frequency distribution of EEDC recordings. Figure 3 shows the 1990 EEDC frequency distribution for Bilthoven (627), which may be considered representative for the situation in the Netherlands. This distribution is normalised and converted to the ambient dose rate by applying a conversion coefficient,  $C_{\text{EEDC}}$ , equal to  $0.5 \text{ nSv}\cdot\text{h}^{-1}\cdot\text{Bq}^{-1}\cdot\text{m}^3$ <sup>(1,3,4)</sup>. Similarly shaped distributions were found at other NRM sites<sup>(4,15)</sup>. Apart from a discrepancy near zero, which is not very relevant because the influence of this part of the EEDC data on the dose rate is insignificant, the shape of such a distribution is fairly well described by a normalised 'one parameter' function,  $A(\gamma)$ :

$$A(\gamma) = q e^{-q\gamma} \text{ for } (\gamma \geq 0)$$

and

$$A(\gamma) = 0 \text{ for } (\gamma < 0) \quad (2)$$

The mean value of this probability density function,  $\gamma_A$ , is calculated as:

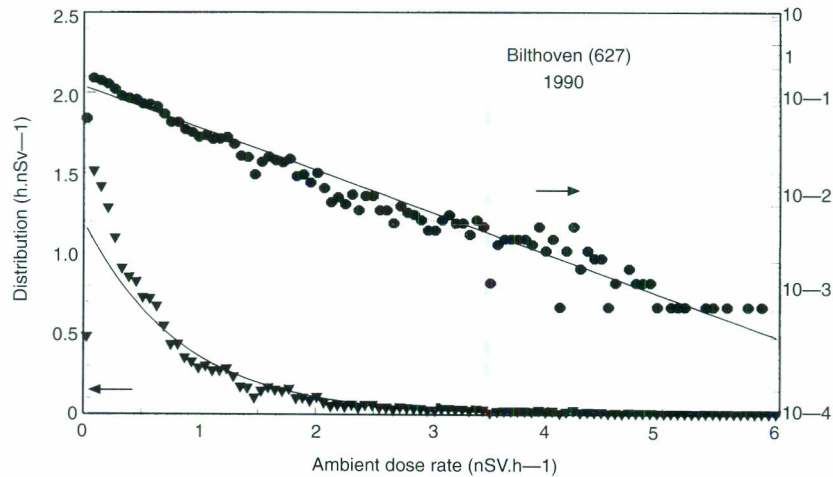


Figure 3. Normalised frequency distribution illustrating the contribution of airborne  $^{222}\text{Rn}$  progeny on the dose rate. The distribution, shown on linear (triangles) and logarithmic scales (circles), is obtained by converting observed EEDC data by a factor of  $0.50 \text{ nSv}\cdot\text{h}^{-1}\cdot\text{Bq}^{-1}\cdot\text{m}^3$ . The histogram data are compared with exponential probability density functions (Equation 2), with  $q$  values derived from the mean (solid lines,  $q = 1.2 \text{ h}\cdot\text{nSv}^{-1}$ ) and median (dashed lines,  $q = 1.3 \text{ h}\cdot\text{nSv}^{-1}$ ) EEDC found for Bilthoven (627) in 1990.

$$\gamma_A = \frac{\int_0^{\infty} \gamma A(\gamma) d\gamma}{\int_0^{\infty} A(\gamma) d\gamma} = q \int_0^{\infty} \gamma e^{-q\gamma} d\gamma = \frac{1}{q} \quad (3)$$

The median of this distribution,  $\gamma_{\text{median}}$ , follows from:

$$\int_0^{\gamma_{\text{median}}} q e^{-q\gamma} d\gamma = 0.50$$

$$\Rightarrow \gamma_{\text{median}} = \frac{\ln 2}{q} = \ln 2 \gamma_A \quad (4)$$

Values for  $q$  can thus be estimated from the annual mean or median values of airborne radioactivity concentrations, for instance, as reported in regular NRM data reports<sup>(16–19)</sup>. The  $q$  values obtained for Bilthoven (627), derived from the mean (1.5 Bq.m<sup>-3</sup>) and the median (1.2 Bq.m<sup>-3</sup>) EEDC values found in 1990, are 1.3 and 1.2 h.nSv<sup>-1</sup>, respectively; the corresponding probability density functions (shown in Figure 3) agree with the Bilthoven 1990 data distribution, except for EEDC data close to zero. Values of  $q$  computed for this location from annual EEDC distributions over the period 1990–1995 vary in the range 0.9–1.8 h.nSv<sup>-1</sup>, with a mean value of 1.3 h.nSv<sup>-1</sup>. Similar results obtained for other NRM locations show a typical discrepancy of 10% between  $q$  values computed from either mean or median EEDC values, indicating that the proposed probability density function is just an approximation. Based on all the NRM locations (14) and years (6) where EEDC data have been collected so far, the shaping parameter  $q$  is found to vary between 0.6 and 2.5 h.nSv<sup>-1</sup> in the Netherlands (location being the most sensitive parameter), with a typical value of 1.2 h.nSv<sup>-1</sup>.

### Wet deposition

The highest temporal increase of ambient dose rate in the Netherlands caused by natural processes comes from rainfall due to the washout of short-lived decay products of <sup>222</sup>Rn. Dose rate elevations related to rainfall can be computed, using an actual time-series of precipitation rate and EEDC as input<sup>(3,4)</sup>. Although this equation is easy to use in explaining or predicting elevated dose rate in a given situation, it is too complex to render the 'long-term' probability distribution of elevated dose rate due to rainfall. Instead, the expression for the probability density function for deposition,  $D(\gamma)$  presented here is derived semi-experimentally.

A probability density function for deposition fairly similar to the one presented in Equation 2 was derived from analysing high dose rate tails observed in actual frequency distributions with, however, one modification. In the case of airborne radioactivity, the same parameter,  $q$ , was used both to determine the slope of the distribution and to normalise the probability density function to 1. In the case of wet deposition, a different

normalisation factor has to be used to match the observed data with the suggested probability density. The reason for this is obvious: most of the time the ambient dose rate is not affected by rainfall at all as it rains as much as 7% of the year in the Netherlands<sup>(12)</sup>. Moreover, deposited daughters of <sup>222</sup>Rn contribute to the ambient dose rate for just a few hours after the rain has stopped. When considering wet periods only, probable dose rate elevations can be characterised by a distribution similar to Equation 2. During the rest of the time the contribution from wet deposition is virtually zero. The following normalised probability density function,  $D(\gamma)$ , is therefore suggested:

$$D(\gamma) = \frac{r-p}{r} \delta(\gamma) + p e^{-r\gamma} \text{ for } (\gamma \geq 0)$$

and

$$D(\gamma) = 0 \text{ for } (\gamma < 0) \quad (5)$$

The delta function introduced in this equation ensures proper normalisation to unity. As will be shown later on, the normalisation and slope parameters  $p$  and  $r$  can be determined from the high tail of the experimentally observed frequency distribution.

### Joint probability density function

The dose rate probability density functions for airborne radioactivity,  $A(\gamma)$ , and wet deposition,  $D(\gamma)$ , contain very similar elements. Applying Equation 1 to these functions results in the following 'sum' function,  $Z(\gamma)$ :

$$Z(\gamma) = C_q e^{-q\gamma} + C_r e^{-r\gamma} \text{ for } (\gamma \geq 0)$$

and

$$Z(\gamma) = 0 \text{ for } (\gamma < 0) \quad (6)$$

with constants  $C_q$  and  $C_r$  equal to:

$$C_q = q \left( \frac{p}{r-q} + \frac{r-p}{r} \right)$$

and

$$C_r = \frac{pq}{q-r} \quad (7)$$

Merging the functions  $S(\gamma)$  and  $Z(\gamma)$  to the final joint ambient dose rate probability density function,  $F(\gamma)$ , follows in a straightforward manner from mathematics:

$$F(\gamma) = C_q \exp \left[ q \left( \gamma_s + \frac{q\sigma_s^2}{2} \right) \right] e^{-q\gamma} \frac{\text{Erfc}[\Phi_q(\gamma)]}{2}$$

$$+ C_r \exp \left[ r \left( \gamma_s + \frac{r\sigma_s^2}{2} \right) \right] e^{-r\gamma} \frac{\text{Erfc}[\Phi_r(\gamma)]}{2} \quad (8)$$

with  $\text{Erfc}(x)$  the complementary error function defined as<sup>(20)</sup>:

$$\text{Erfc}(x) = \frac{2}{\sqrt{\pi}} \int_x^{\infty} e^{-t^2} dt \quad (9)$$

The  $\gamma$ -dependent arguments of the complementary error function in Equation 8,  $\phi_q(\gamma)$  and  $\phi_r(\gamma)$ , are given by:

$$\phi_q(\gamma) = \frac{\gamma_s + q\sigma_s^2 - \gamma}{\sigma_s \sqrt{2}}$$

and

$$\phi_r(\gamma) = \frac{\gamma_s + r\sigma_s^2 - \gamma}{\sigma_s \sqrt{2}} \quad (10)$$

The high tail of  $F(\gamma)$  can be approximated as follows: if  $\phi_q(\gamma) < -2$  then  $\text{Erfc}(\phi_q(\gamma)) \approx 2$ . From Equation 10 it follows that this condition is true if  $\gamma > \gamma_s + \Delta\gamma$ , with  $\Delta\gamma = 2(2\sigma_T + q\sigma_T^2)^{1/2}$  (typically  $10 \text{ nSv.h}^{-1}$ ). Because  $r < q$ ,  $\phi_r(\gamma) < \phi_q(\gamma)$ , the condition  $\phi_q(\gamma) < -2$  also implies that  $\phi_r(\gamma) < -2$  and  $\text{Erfc}(\phi_r(\gamma)) \approx 2$ . For large values of  $\gamma$ , Equation 8 is thus approximated as:

$$F(\gamma) \approx C_q \exp\left[q\left(\gamma_s + \frac{q\sigma_s^2}{2}\right)\right] e^{-q\gamma} + C_r \exp\left[r\left(\gamma_s + \frac{r\sigma_s^2}{2}\right)\right] e^{-r\gamma} \quad (\gamma > \gamma_s + \Delta\gamma) \quad (11)$$

By substituting the condition for  $\gamma$  in Equation 11 and making use of the fact that  $r < q$ , it can be easily shown that the first term of this function can be ignored. After rewriting, the high tail of the joint dose rate probability density function is approximated by:

$$F(\gamma) \approx p \exp[-r(\gamma - \gamma_s - \delta\gamma)]$$

$$(\gamma > \gamma_s + \Delta\gamma) \quad \text{with} \quad \delta\gamma = \frac{r\sigma_s^2}{2} + \frac{\ln\left(\frac{q}{q-r}\right)}{r} \quad (12)$$

In comparing Equation 12 with Equation 5 it becomes clear that, for large  $\gamma$  values, the joint probability density function,  $F(\gamma)$ , represents the corresponding probability density function for wet deposition,  $D(\gamma)$ , but translated over a distance  $\gamma_s + \delta\gamma$ , with  $\delta\gamma$  typically being  $1.0\text{--}1.5 \text{ nSv.h}^{-1}$ , which is small compared to  $\gamma_s$ . Parameters for describing likely contributions to the ambient dose rate due to rainfall can indeed be derived from the high dose rate tail of a frequency histogram. Examples of the functions  $S(\gamma)$ ,  $Z(\gamma)$  and  $F(\gamma)$  are plotted in Figure 4.

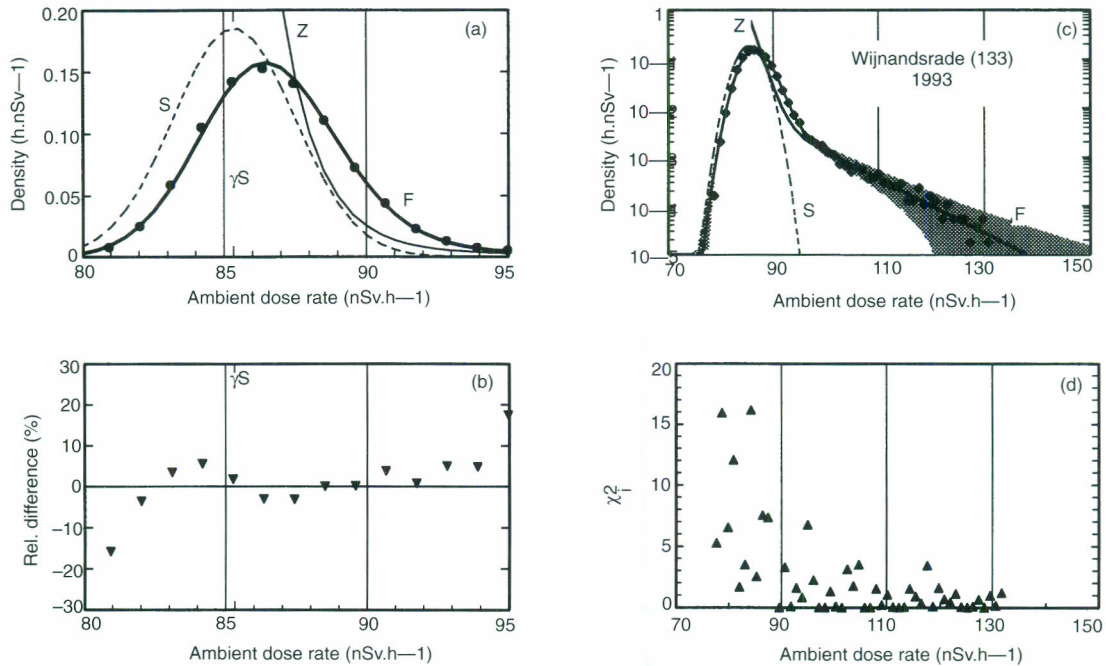


Figure 4. Comparison of the derived probability density function,  $F(\gamma)$ , and the experimental data distribution obtained for Wijnandsrade (133) in 1994 on linear (a) and logarithmic scales (c). The intermediate probability density functions  $S(\gamma)$  and  $Z(\gamma)$  are also indicated, the latter translated over a distance of  $\gamma_s$ . At high dose rates the shape of  $F(\gamma)$  is dominated by the contribution from wet deposition. The shaded area in (c) indicates the 95% confidence interval for the statistical scattering of individual histogram data. (b) (relative difference) and (d) ( $\chi^2_i$  values) provide indicators for the goodness of fit.

## RESULTS

Twenty-five annual frequency distributions, obtained from NRM sites located in the middle, the north-east, the south-east, the south-west and the western part of the Netherlands were analysed over the period 1990–1994. On four occasions dose rate distributions were strongly disturbed due to frequent malfunction of equipment or human interference and had to be excluded from the test<sup>(4)</sup>.

Location-dependent annual average values of air pressure<sup>(21)</sup> and EEDC<sup>(16–19)</sup> were applied to calculate the input parameters  $\gamma_C$  and  $q$ . The parameter  $\sigma_C$  was calculated, assuming a fixed air pressure standard deviation,  $\sigma_p$ , equal to 10 hPa. The standard deviation due to counting noise,  $\sigma_N$ , was calculated using a fixed value for the parameter  $N_0$  of 29 counts per nSv.h<sup>-1</sup> per 10 min counting interval. The parameters  $p$  and  $r$  were fitted from the high tail of the data distribution, while the parameters  $\gamma_T$  and  $\sigma_T$  were adjusted to match the joint probability density function with the top and the lower half of the histogram.

Calculated and measured values extend over a range of four orders of magnitude. Two quantities were used to adjust the free parameters and to evaluate the goodness of fit. Around the top of the distribution some  $10^2$ – $10^5$  data are recorded per interval per year, showing good statistics. In this region the relative difference between the joint probability density function and the normalised histogram was evaluated. Away from the top, especially at the high tail of the distribution, just a few (say <100) recordings are expected per interval per

year and statistical scattering becomes important. To examine the goodness of fit for those parts of the distribution  $\chi_i^2$  values, defined as<sup>(22)</sup>:

$$\chi_i^2 = \frac{[F(\gamma_i) - H(\gamma_i)]^2}{N F(\gamma_i)} \quad (13)$$

were considered. In Equation 13  $F(\gamma_i)$  is the normalised probable value at dose rate  $\gamma_i$  (Equation 8),  $H(\gamma_i)$ , the measured (normalised) histogram value around midpoint  $\gamma_i$ , and  $N$ , the total number of data involved. For sampling times of 10 min,  $N$  is approximately  $5 \times 10^4$  for a time period of one year and a typical data availability of 95%.

Figure 4(a–d) illustrates the outcome of this analysis by showing the 1993 results obtained for Wijnandsrade (133). This location exhibits the highest concentrations of airborne radioactivity of all NRM monitoring sites<sup>(4,15)</sup> and is thus most pronounced in its variations in ambient dose rate. Figure 4(a) compares the top area of the proposed joint probability function and the normalised frequency distribution on a linear scale; their relative differences are shown in Figure 4(b). The small mismatch observed at the top (histogram data are shifted slightly to the left), originating from assuming a normal air pressure distribution, is also noticed in other results. In fact, the air pressure distribution is often slightly asymmetric, with a shorter wing in the high and a longer wing in the low air pressure region. In Figure 4(a), we see a reverse profile in the experimental data due to the negative correlation between cosmogenic dose rate and air pressure. This feature also explains the fairly high

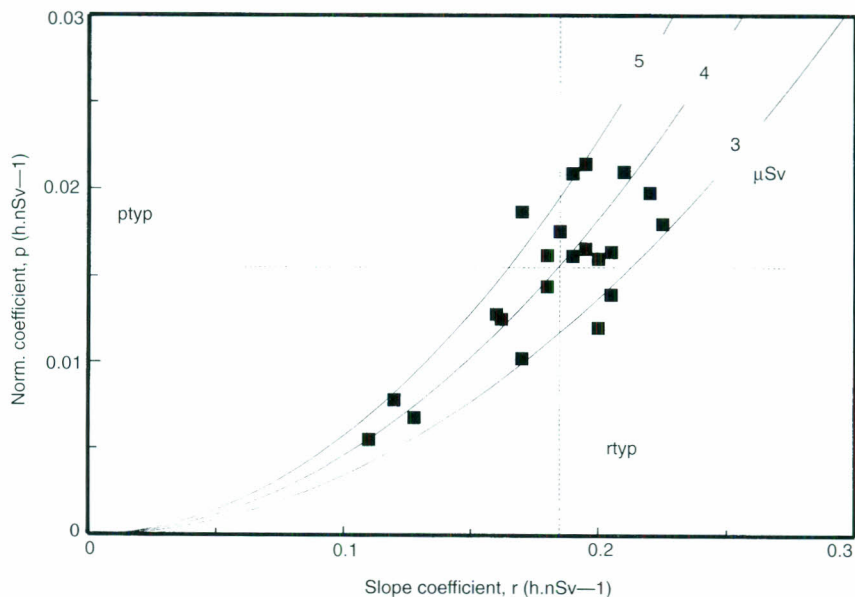


Figure 5. Combinations of  $p$  and  $r$  derived from the analysis of 21 dose rate histograms. Typical parameter values are presented by dashed lines. The three solid parabolic lines connect pairs of  $p$  and  $r$  yielding the same annual dose due to rainfall, as indicated.

$\chi^2$  values observed below  $90 \text{ nSv.h}^{-1}$  (Figure 4(d)). Figure 4(c) compares the joint probability density function with the histogram data on a logarithmic scale. Below  $2 \times 10^{-3}$  (i.e. approximately 100 or fewer likely recordings per interval per year) the statistical scattering of data becomes important. The shaded area provides an estimate of the  $2\sigma$  probability range for individual histogram data, assuming  $\sigma_i^2$  being equal to  $N F(\gamma_i)$ .

Best estimates for the parameters expressing the influence of rainfall, i.e.  $p$  and  $r$ , show considerable variations (see Figure 5), both in location and time. Variations between years reflect the variable character of weather conditions, while spatial variations are merely due to differences in local ground surface characteristics. These influence the ambient dose rate following a given deposition of radionuclides. Mean and median values found for  $p$  are  $0.015$  and  $0.016 \text{ h.nSv}^{-1}$ , respectively; for  $r$  these values were found to be  $0.18$  and  $0.19 \text{ h.nSv}^{-1}$ , respectively. Typical values, as indicated in Figure 5, were taken in between. The quotient of the latter, i.e.  $p_{\text{typ}} r_{\text{typ}}^{-1}$ , equals  $8.4 \times 10^{-2}$ . Ambient dose rate is thus on the average influenced by rainfall for approximately 8.5% of the time. Being slightly higher than the average period of rainfall in the Netherlands, which is 7% in the long term<sup>(12)</sup>, this value agrees with the expected value. The annual ambient dose due to the washout and rainout of  $^{222}\text{Rn}$  progeny, computed from the typical parameter values for  $p$  and  $r$ , equals  $4 \mu\text{Sv.a}^{-1}$ . Taking a precipitation rate of  $800 \text{ mm.a}^{-1}$ , as normally observed in the Netherlands<sup>(12)</sup>, the time-integrated ambient dose following one unit of precipitation is, on average,  $5 \text{ nSv.mm}^{-1}$ . This value compares to the  $4.1 \text{ nSv.mm}^{-1}$  derived from the analysis of individual rain showers at Bilthoven (627)<sup>(3,4)</sup>. Rainfall may occasionally lead to highly elevated recordings of ambient dose rate, but the total impact from this source is

very small; it contributes less than 1% to the total time-integrated ambient dose. This contribution is even less than the average annual contribution of airborne radioactivity to the ambient dose, which is, with  $q$  being typically  $1.2 \text{ h.nSv}^{-1}$ , of the order of  $7 \mu\text{Sv.a}^{-1}$ .

The other parameter of interest,  $\sigma_T$ , expressing the temporal variation in the terrestrial dose rate contribution, ranges from virtually zero to  $1 \text{ nSv.h}^{-1}$ . Some of the higher values, however, are probably overestimated due to factors like changes in the built-up surroundings and replacement of equipment not accounted for in the present description. On the other hand, NRM equipment underestimates the terrestrial dose rate by some 10%<sup>(4)</sup>. The mean and median values derived from this test, with  $0.67$  and  $0.75 \text{ nSv.h}^{-1}$  close to each other, are therefore considered representative. Temporal variations in terrestrial radiation are thus, in general, confined to a range of  $\pm 2 \text{ nSv.h}^{-1}$  in the Netherlands. A similar result was found from the analysis of monthly averaged data for the 14 principal NRM locations over the period 1990–1994<sup>(3,4)</sup>.

In Table 1, typical values to describe the influences of various sources on the ambient dose (rate) in the Netherlands are summarised. Some of the figures in this table, such as the typical value for  $\gamma_T$ , were taken from related studies not evaluated in this paper.

## DISCUSSION AND CONCLUSIONS

Frequency distributions of ambient dose rate data, as observed by the Dutch National Radioactivity Monitoring Network, were shown to be well described by considering only five (virtual) sources and processes using simple expressions for the likelihood of their occurrence. Over one million data pairs, obtained from various locations and years, were used in this analysis, of

**Table 1. Parameter values (best estimates) and derived quantities characterising source-dependent contributions to the ambient dose equivalent rate ( $\dot{H}^*(10)$ ) in the Dutch outdoor environment.**

Source	Probability density function	Shape parameters		Average dose rate (nSv.h <sup>-1</sup> )	Annual dose (μSv.a <sup>-1</sup> )	Rel. dose (%)
		$\gamma_X(\text{nSv.h}^{-1})$	$\sigma_X(\text{nSv.h}^{-1})$			
Cosmogenic	normal	40	1.2	40	350	49
Terrestrial <sup>(a)</sup>	normal	40	0.7	40	350	49
Counting Noise <sup>(b)</sup>	normal	0	1.6	— <sup>(c)</sup>	— <sup>(c)</sup>	— <sup>(c)</sup>
		$p \text{ (h.nSv}^{-1}\text{)}$	$q, r \text{ (h.nSv}^{-1}\text{)}$			
Airborne r.a. <sup>(d)</sup>	exp. decay	— <sup>(c)</sup>	1.2	0.8	7	1
Deposited r.a.	exp. decay	0.016	0.19	5.3 <sup>(e)</sup>	4	0.6

<sup>(a)</sup>Location-dependent; range in the Netherlands:  $15\text{--}75 \text{ nSv.h}^{-1}$ .

<sup>(b)</sup>Considered as a 'virtual' zero-mean source; values are for NRM equipment, sampling time 10 min.

<sup>(c)</sup>Not applicable.

<sup>(d)</sup>Average EEDC in the Netherlands (over the period 1990–1995):  $1.7 \text{ Bq.m}^{-3}$ .

<sup>(e)</sup>Only during 'wet' periods (typically 8.5% of the year).

which the results are considered representative for the Netherlands. Cosmogenic and terrestrial radiation together account for over 98% of the total dose rate; their contributions are represented by normal functions with mean values, both in the order of 40 nSv.h<sup>-1</sup>. Their temporal variations, due to variations in air pressure and radon soil profile, are expressed by standard deviations of 1.2 and 0.7 nSv.h<sup>-1</sup>, respectively. The measured frequency distribution is broadened due to counting statistics; for the NRM set-up the corresponding standard deviation is typically 1.6 nSv.h<sup>-1</sup> for a 10 min sampling time. These three sources add up to a normal distribution with a location-dependent mean value in the range 50–120 nSv.h<sup>-1</sup> and a standard deviation of typically 2.1 nSv.h<sup>-1</sup>. On average, airborne and deposited short-lived decay products of <sup>222</sup>Rn have a low impact on the natural background radiation (i.e. ≤1% each) but their contributions can occasionally lead to significant dose rate elevations. In both cases the likelihood of their dose rate contribution is expressed by an exponential function, stating that the probability of a certain contribution decreases exponentially with increasing dose rate. In the case of washout of <sup>222</sup>Rn progeny, this exponential probability was found to be present for approximately 8.5% of the year. In the remaining period the contribution from this source is zero.

In our approach it is assumed that sources and processes under consideration are not correlated. In fact, some correlation does exist, for instance, between air pressure and EEDC, and air pressure and precipitation; however, these correlations were found to be rather weak<sup>(4)</sup>. Apparently, the assumption of uncorrelated sources works well, since calculated and experimental results agree over four orders of magnitude.

The analysis presented here was carried out using data obtained in the Netherlands. Therefore, one should be cautious in applying the resulting parameter values

to regions with strongly deviating environmental characteristics. Also, the applied measuring method and equipment may have influenced the results. Slightly different parameter values may be needed to match the proposed description with frequency distributions recorded when applying a different experimental set-up. To give one example, the ambient dose rate due to surface radioactivity decreases with increasing sampling height and calculations obtained from the dose rate model Soil\_Rad<sup>(8)</sup> show that the dose rate from deposited radon progeny at 3.5 m equals approximately 95% of the dose rate expected at 1 m sampling height. The rainfall parameters  $p$  and  $r$  are thus a function of sampling height: in this example expected values for these parameters at 1 m sampling height are  $p_{1m} = p_{3.5m}/0.95$  and  $r_{1m} = r_{3.5m}/0.95$ , as is simply derived from the applied probability density function. Such values cause a longer tail in the data distribution.

This study yields quantified knowledge on the probability of temporal variations in ambient dose rate due to natural causes, which can serve in the management of nuclear emergency networks. The ranges and likelihood of dose rate variations presented here can be used to establish proper warning levels, where it is important to find a precise balance between sensitive detection of radiological accidents and occasional false alarms caused by fluctuations of natural background levels<sup>(1,2)</sup>. This kind of information can also facilitate the validation of data and the control of equipment, thus supporting the quality assurance of the network.

#### ACKNOWLEDGEMENTS

The authors thank Professor Dr A. van der Woude and Professor Dr R. J. de Meijer (Groningen University/KVI) for stimulating comments and discussion and also their colleagues at the RIVM for their loyal assistance.

#### REFERENCES

1. Smetsers, R. C. G. M. and Blaauboer, R. O. *Time-Resolved Monitoring of Outdoor Radiation Levels in the Netherlands*. Radiat. Prot. Dosim. **55**(3), 173–181 (1994).
2. Smetsers, R. C. G. M. and Lunenburg, A. P. P. A. van. *Evaluation of the Dutch Radioactivity Monitoring Network for Nuclear Emergencies over the Period 1990–1993*. Radiat. Prot. Dosim. **55**(3), 165–172 (1994).
3. Smetsers, R. C. G. M. and Blaauboer, R. O. *A Dynamic Compensation Method for Natural Ambient Dose Rate based on 6 Years Data from the Dutch Radioactivity Monitoring Network*. Radiat. Prot. Dosim. **69**(1), 19–31 (1997) (This issue).
4. Blaauboer, R. O. and Smetsers, R. C. G. M. *Variations in Outdoor Radiation Levels in the Netherlands*. Thesis, University of Groningen (Groningen) (1996).
5. Smetsers, R. C. G. M. *An Automated Airborne Gross- $\alpha/\beta$  Monitor applied to Time-resolved Measurements of <sup>222</sup>Rn Progeny Concentrations in the Air*. Health Phys. **68**(4), 546–552 (1995).
6. Bitt Technology. *Radiation Monitor RM10 — Gammasonde RS02 (Technisches Manual)* (Bitt Technology, Spillern) (1988).
7. International Commission on Radiation Units and Measurements. *Measurement of Dose Equivalents from External Photon and Electron Radiations*. Report 47 (Bethesda, MD: ICRU Publications) (1992).
8. Blaauboer, R. O. *SOIL\_RAD, a Computer Program to Calculate Air Kerma, Ambient Dose Rate and Effective Dose Rate due to Photons emitted by Radionuclides Distributed in Soil or on the Soil-Air Surface*. (National Institute of Public Health and the Environment, Bilthoven) RIVM Report no. 610064001 (1995).
9. Frenzel, E. *Umgebungsüberwachung mit dem Aerosol-Monitor FHT 59 S*. (Manual) (FAG Kugelfischer Georg Schäfer KGaA, Erlangen) (1991).

10. Knutson, E. O. *Modeling Indoor Concentrations of Radon's Decay Products*. In: Radon and its Decay Products in Indoor Air. Eds W. W. Nazaroff and A. V. Nero (New York: Wiley) pp. 161–202 (1988).
11. UNSCEAR. *Sources, Effects and Risks of Ionizing Radiation*. (Annex A). UNSCEAR report 1993 (New York: United Nations) (1993).
12. KNMI. *Climatological Data of Stations in the Netherlands. Normals and Extreme Values of the 15 Principal Stations for the Period 1961–1990*. Royal Netherlands Meteorological Institute, De Bilt. Publication no. 150-27 (1992).
13. Strandén, E., Kolstad, A. K. and Lind, B. *Radon Exhalation: Moisture and Temperature Dependence*. Health Phys. **47**(3), 480–484 (1984).
14. Schumann, R. R., Owen, D. E. and Asher-Bolinder, S. *Effects of Weather and Soil Characteristics on Temporal Variations in Soil-gas Radon Concentrations*. Geological Society of America, Special paper 271 (1992).
15. Blaauboer, R. O. and Smetsers, R. C. G. M. *Outdoor Concentrations of the Equilibrium-Equivalent Decay Products of  $^{222}\text{Rn}$  in the Netherlands and the Effect of Meteorological Variables*. Radiat. Prot. Dosim. **69**(1), 7–18 (1997) (This issue).
16. Aldenkamp, F. J., Vries, L. J. de, Lunenburg, A. P. P. A. van, Smetsers, R. C. G. M. and Westerlaak, P. J. M. van. *National Radioactivity Monitoring Network (LMR): Data Report 1990*. National Institute of Public Health and the Environment, RIVM Report no. 749206001, Bilthoven (1992).
17. Kwakman, P. J. M., Aldenkamp, F. J., Vries, L. J. de, Drost, R. M. S., Tijmsmans, M. H., Koolwijk, A. C. and Ockhuizen, A. *Monitoring of Radiation in Atmosphere, Water and a Food Chain. Results in the Netherlands in 1991*. National Institute of Public Health and the Environment, RIVM Report no. 749204004, Bilthoven (1993).
18. Aldenkamp, F. J., Drost, R. M. S., Koolwijk, A. C., Kwakman, P. J. M., Lunenburg, A. P. P. A. van, Ockhuizen, A., Tax, R. B., Tijmsmans, M. H., Vries, L. J. de and Westerlaak, P. J. M. van. *Monitoring of Radiation in Atmosphere, Water and a Food Chain. Results in the Netherlands in 1992*. National Institute of Public Health and the Environment, RIVM Report no. 749204014, Bilthoven (1994).
19. Smetsers, R. C. G. M., Vries, L. J. de, Lunenburg, A. P. P. A. van and Aldenkamp, F. J. *National Radioactivity Monitoring Network (LMR): Data Report 1993–1995*. National Institute of Public Health and the Environment, RIVM Report no. 610056028, Bilthoven (1996).
20. Kreyszig, E. *Advanced Engineering Mathematics* (New York: John Wiley & Sons) (1979).
21. KNMI. *Maand/jaaroverzicht van het weer in Nederland*. 87–91st year, no. 1-13. Royal Netherlands Meteorological Institute, De Bilt (1990–1995).
22. Kreyszig, E. *Introductory Mathematical Statistics* (New York: John Wiley & Sons) (1970).